# Dosimetry with the TruView gel on a 0.35 T MR-Linac: A feasibility study

L. Ermeneux, A. Petitfils, L. Marage, R. Gschwind, Christelle Huet

Radiation Measurements 175 (2024) 107170

Contents lists available at ScienceDirect

Radiation Measurements

journal homepage: www.elsevier.com/locate/radmeas

# Dosimetry with the TruView gel on a 0.35 T MR-Linac: A feasibility study

L. Ermeneux [a,*], A. Petitfils [b], L. Marage [b], R. Gschwind [c], C. Huet [a]

[a] Institut de Radioprotection et de Sûreté Nucléaire (IRSN), Laboratoire de dosimétrie des rayonnements ionisants, Fontenay-aux-Roses, France
[b] Centre Régional de Lutte Contre le Cancer Georges-François Leclerc (CGFL), Dijon, France
[c] Université de Franche-Comté, Laboratoire Chrono-environnement – UMR CNRS 6249, Montbéliard, France

ARTICLE INFO

*Keywords:*
3D gel dosimetry
Fricke gel
MR-Linac

ABSTRACT

The purpose of this work is to assess the feasibility of performing dosimetry with the TruView (ModusQA, London, Ontario, Canada) MTB Fricke gel by MRI reading on a low field MR-Linac (0.35 T). Radiochromic TruView gels were manufactured at IRSN. A 4 echoes time (TE) single-shot fast spin echo sequence (HASTE) was used for 2D images acquisitions. Raw MRI images were denoised (MP-PCA) and transversal relaxation rates (R2) maps were extracted using a homemade Matlab routine. Temperature influences on R2 as well as gel homogeneity were investigated. A dosimetric evaluation of the TruView gel was conducted implying four gels made from the same batch, with three of them dedicated to calibration, and the fourth one received a simple dosimetric plan. Results showed the TruView gel to be sensitive to temperature drift. A protocol was thus developed to ensure thermal stability with the use of a dedicated temperature-controlled water bath. An inhomogeneity that manifests as a R2 increase near the air/gel interface was found to cause a 4% amplitude deviation in R2 along unirradiated gels. Air sealing drastically reduced the inhomogeneity. Dose versus R2 calibration was established. TruView gel sensitivity was found to be low (0.0093 $Gy^{-1}$ $s^{-1}$). 1D and 2D comparison to planned dose distribution displayed overall agreement with global gamma index (5%/3 mm) evaluation with an 87 % passing rate. Main discrepancies in the low and gradient dose regions were attributable to the calibration range and diffusion effects. This study demonstrated the feasibility of using the TruView gel for dosimetric evaluation on a low field MR-Linac. The protocol developed needs to be extended to a full 3D evaluation to enable patient QA and may require modifications to the gel formulation to increase its overall sensitivity and ensure limited dependence on temperature drift.

## 1. Introduction

In recent years, the increasing complexity of radiotherapy treatments has highlighted a growing need for dosimeters that enable robust and reliable three-dimensional dosimetric assessment of doses delivered to the patient. Among the available tools, dosimetric gels are among the few allowing true 3D assessment of dose distributions (De Deene, 2022; Marrale and d'Errico, 2021).

The first dosimetric gels were based on the Fricke solutions containing ferrous ions (Fe2+), oxidating into ferric ions (Fe3+) under irradiation (Fricke and Morse, 1927). In the 1980s, the Yale group demonstrated that the different paramagnetic properties of Fe2+ and Fe3+ ions allowed for a nuclear magnetic resonance (NMR) readout of the delivered dose to these solutions (Gore and Kang, 1984) and that fixing the ions in an agarose gel matrix enables spatial measurement of dose distributions. After Fricke gels, polymer gels were developed whose principles and composition differ from those of Fricke gels described above, but which still allow MRI dose readout. These have undergone accelerated development as they allow spatial conservation of dose distributions over time (Baldock et al., 2010; De Deene, 2022; Marrale and d'Errico, 2021), enabling delayed readings unlike Fricke gels, which are subject to diffusion phenomena (Gore and Kang, 1984; Macchione et al., 2022). Fricke gels as well have undergone improvements in terms of stability through modifications in their gelatinous matrix and the addition of chelating agents to their composition (Rae et al., 1996; Scotti et al., 2022). These gels are non-toxic, simple to manufacture, and cost-effective, making them particularly attractive for dosimetric evaluation.

However, these dosimeters are currently under-utilized in clinical routine due to the overall reliability limitations of the technique, implementation difficulties, and lack of easy access to imaging systems for their readout. Active research in the field of gel dosimetry has sought

* Corresponding author.
*E-mail address:* louis.ermeneux@gmail.com (L. Ermeneux).

https://doi.org/10.1016/j.radmeas.2024.107170
Received 15 January 2024; Received in revised form 26 April 2024; Accepted 16 May 2024
Available online 17 May 2024

to substitute the original MRI-based readout method with techniques based on the utilization of CT (Hilts, 2006; Hilts et al., 2000; Javaheri et al., 2020; Jirasek et al., 2020) and optical scanners (Chou et al., 2020; Colnot et al., 2018; da Silveira et al., 2022; Doran et al., 2001; Gore et al., 1996; Oldham et al., 2001). However, despite the performances of optical techniques reading, and the accessibility of the CT reading modality, the use of gel dosimetry for patient quality control is not yet widespread.

Presently, the integration of machines equipped with onboard magnetic resonance imagers within radiotherapy clinics holds the promise of providing physicist with readout device within a reasonable timeframe (Baldock et al., 2020). To date, there are two MR-Linac systems implemented in radiotherapy centres: the Unity system from Elekta, with a 1.5 T magnet MRI (Raaymakers et al., 2017), and the MRIdian system from ViewRay (Paolo Alto, CA, USA), generating a 0.35 T magnetic field (Klüter, 2019). In MRI gel dosimetry, the signal-to-noise ratio (SNR) of the acquired images is an important factor as the precision of the converted dose maps directly depends on it. This ratio is directly proportional to the MRI static magnetic field intensity. Therefore, most dosimetric gel studies have mainly involved the use of diagnostic MRI, where the static magnetic field intensity typically ranges between 1.5 T and 3 T. Performing dosimetric measurements on a low-field MRI poses a challenge that few studies have reported to date (Baldock et al., 2020). Furthermore, these studies are based on the use of polymer gels (Dorsch et al., 2019; Elter et al., 2022; Marage et al., 2022; Maraghechi et al., 2020), and none have addressed Fricke gels to our knowledge.

The aim of the present study is to assess the feasibility of reading the TruView (ModusQA) MTB Fricke gels with the low-field MRI of the MRIdian for dose distribution assessment.

## 2. Materials and methods

### 2.1. Gels manufacturing

The TruView gels used in this study were homemade using the formulation provided by ModusQA (Penev and Mequanint, 2015, 2017). Its composition is based on Fricke solutions with ferrous ion concentration at 0.1 Mm, sulfuric acid at 35 mM, 5-nitro-1,10-phenanthroline (0.3 mM), glyoxal (5 mM), and a low diffusion gelatin matrix (4 %). The TruView gel includes the addition of a chelating agent, MethylThymol Blue (MTB) at 0.1 mM concentration, which reacts with ferric ions in the solution to form Fe3+-MTB complexes, inducing changes in the absorption domain that allows optical reading. Several studies have investigated the performance of TruView gel, evaluating its properties through optical reading and demonstrating good water equivalence and weak energy and dose rate dependence (Colnot et al., 2017, 2018). A maximum of 2 L were produced at a time, and the gels were packaged in transparent cylindrical jars of 1 l or 400 ml depending on the investigation (Fig. 1). The jars were covered with aluminium foil and stored in a fridge at 4 °C at least 4 days before use to allow the gel to fix and chemically stabilize.

### 2.2. Reading and analysis

The MRIdian MR imager produces a 0.35 T low static magnetic field with a homogeneous region 50 cm in diameter. Predefined MRI sequences with manageable parameters are available on the MRIdian system. Signal reception was achieved using two Viewray 2 × 6 channels torso surface coil arrays. A T2-weighted single-shot fast spin echo sequence (HASTE) was used in this study. The reason for performing T2 rather than T1 measurements for this study lies, on the one hand, in the limited number of predefined T1-weighted fast sequences available on the MRIdian and, on the other hand, in the artifacts obtained with the IR-EPI (inversion recovery) sequence and the low SNR of the SPGR sequence (spoiled gradient). The HASTE sequence enables complete

**Fig. 1.** TruView gel from the same batch packaged in three 400 ml cylindrical jars partially filled.

images to be acquired in a single repetition time (TR) and does not lead to the behaviours encountered when using T1-weighted sequences, providing good image SNR with limited artifacts. The HASTE sequence parameters were fixed based on previous investigation intending to optimize it in terms of signal-to-noise ratio by assessing the $T2_0$ values of the unirradiated TruView gel and fixing TE and TR according to it. TR was set at 6000 ms and a total of 4 images were acquired in a single shot with effective echo time (TEeff) of 32, 640, 1240, 1840 ms. Number of signal average was set to 8 to increase SNR, and the corresponding total acquisition time was 48 s. The field of view (FOV) was defined to 350 × 350 $mm^2$ with a voxel size of 2.5 × 2.5 × 10 $mm^3$ for the dosimetric and homogeneity investigation, and to 1.25 × 1.25 × 10 $mm^3$ for the thermal sensitivity assessment.

An in-house MATLAB routine was used to obtain the corresponding spin-spin relaxation rate (R2) maps. Raw MRI images were pre-processed to reduce noise by applying a MP-PCA filter (Olesen and Jespersen, 2020). These processed images were used to generate R2 maps by performing a voxel-by-voxel exponential decay fitting on the processed MRI images acquired at the 4 different echo time values.

### 2.3. Study of unirradiated gels

#### 2.3.1. Thermal sensitivity assessment

The temperature dependence of the relaxation rate (R2) was investigated. The gels were removed from the fridge the day before the measurements to reach room temperature, as established in the protocol developed by Colnot (Colnot et al., 2017). A water bath was used, and its temperature was monitored using a probe thermometer and adjusted to be within ±0.2 °C of room temperature. Two different protocols were followed:

- one jar was stabilized at room temperature (20.5 °C) before MRI-reading and was then placed in the water bath for MRI-reading;
- a second jar was positioned in the water bath 3 h before performing MRI reading (room temperature at 20.2 °C).

Fig. 2 shows the full setup configuration before entering the MRI bore. Then, MRI acquisitions of each jar separately were performed at 5 min time intervals for a duration of 1h15min. Quantitative assessment of R2 changes in the gels was performed by selecting regions of interest (ROIs) of 7 voxels along the gel horizontal axis at a depth of 3 cm.

#### 2.3.2. Gel homogeneity

Gel homogeneity was assessed by acquiring MRI images of unirradiated gel jars filled to a height of 9 cm. R2 inhomogeneity in the

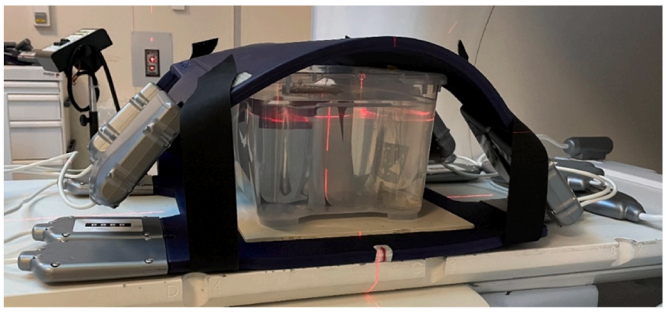

**Fig. 2.** Setup configuration for thermal sensitivity assessment, gel is positioned into the water bath and surface coils are placed under and over the system for signal reception.

direction of gel depth was observed, with an increase in R2 from the air/gel surface to around 12 mm depth, followed by a decrease to 6 cm depth and finally a stabilization before a slight increase at the gel/jar interface. Its origin has been investigated. First, the influence of gel's positioning and orientation within the field was assessed. Images of a jar filled with gel to a height of 9 cm were acquired for different jar orientations (rotations around the point located in the centre of the jar at a depth of 3 cm in the gel): 0°, 90°, 180° and 270°. R2 measurements were also performed for the jar at different positions: from −6 cm et + 6 cm in the X direction and from −10 cm to +10 cm in the X direction by step of 2 cm. Secondly, a potential effect of gel's conditioning was evaluated. A first test consisted in comparing the R2 maps of two jars filled up to a height of 9 cm, but one of which had been solidified upside down (i.e. the jar had been rotated 180° just after gel filling). In a second, test, the R2 map obtained for a partially filled jar was compared with that obtained for a fully filled jar sealed to air by applying a plastic film between the gel surface and the lid.

### 2.4. Dosimetric evaluation

Dosimetric performance of the TruView gel was conducted using four gel jars from the same batch. Gels were packaged in 400 ml jars, fully filled, sealed to air, and stabilized in a water bath for a period of 3-h prior to measurements. The gels were then placed out of the water bath aligned on the lower surface coil and with the upper coil in direct contact with the jar lid. Pre-reading was performed to enable background subtraction from the R2 maps. MRI images of the gel jar were imported into the MRIdian treatment planning system (TPS). As the MRI images lacked inherent electron densities, dosimetric calculations were performed after segmentation of the gel volume and assignment of water's electron density. Each of the four gels was irradiated individually on the MR-Linac according to treatment planning. Three gels were used for calibration purposes and were irradiated at 3 Gy, 5 Gy, and 7 Gy respectively, at a depth of 6 cm in the gel with the MRIdian gantry at 0° and a field size of 3.32 × 3.32 $cm^2$. The fourth gel was used to deliver a simple plan, consisting of five beams of 3.32 × 3.32 $cm^2$ with the gantry at 90°, 35°, 0°, 270° and 315° respectively delivering a total of 5 Gy to the isocentre. After irradiation, images were acquired with all four gels replaced aligned in the bore. Readings were performed strictly 1 h after irradiation, and acquisitions were repeated 10 times. $R2_B$ and R2 maps were then extracted from pre and post irradiation MR images and ΔR2 maps were obtained from background subtraction ($R2-R2_B$). Calibration was carried out using the method proposed by Oldham (Oldham et al., 1998), consisting in adjusting the ΔR2 depth dose measured in the first three gels to depth dose values predicted by the TPS. This calibration process aims to generate more data points than a single measured ROI and is performed with a smaller quantity of calibration vials, thus reducing the overall duration of the dosimetric protocol. A linear ΔR2/dose function was established. The ΔR2 maps were converted to dose maps and a 1D dosimetric evaluation was performed on the fourth gel. The measured dose profiles were compared with the planned dose profiles by a local gamma evaluation with a criterion of 3%/3 mm, this criterion being commonly used for the evaluation of IMRT plans. Next, a 2D validation compared the dose distribution to the planned TPS dose distribution, using both global and local gamma with a criterion set at 5%/3 mm, the dose criterion was increased as it was identified as a major source of discrepancy in plan evaluation. To ensure accuracy, the gel region located 1 cm from the jar wall was removed for 2D evaluation to eliminate potential artifacts in that region.

## 3. Results and discussion

### 3.1. External parameters dependence assessment

#### 3.1.1. Thermal stability

Fig. 3 shows the variation of the gels' transverse relaxation rate (R2) over time for a gel stabilized in air at room temperature and one stabilized at room temperature in a water bath 3 h before measurements, relative to the first measured value. In the case of the air-stabilized gel, a decrease in R2 over time is observed and evaluated at 8.7% ± 1.7% 75 min after the first measurement. This decrease in R2 over time corresponds to an elongation of T2 and therefore to the existence of a warming effect. For the gel previously stabilized in water, the variations observed are not significant (maximum amplitude at 0.3% ± 1.0%). Studies have also revealed a similar sensitivity of this type of gel by optical readout, where changes were observed depending on its irradiation temperature (Colnot et al., 2017). In the case of MRI readout, the specific sensitivity of hydrogels to temperature is mainly linked to the strong presence of water molecules in their composition, whose Larmor precession frequency depends linearly on temperature (Turner and Streicher, 2012). This particular sensitivity of gels to temperature is reflected in the MRI readout by changes in relaxation rates, potentially leading to errors in dosimetric analyses (De Deene and De Wagter, 2001). The protocol for stabilizing the gel in temperature prior to measurements seems effective since no significant R2 variation was observed.

#### 3.1.2. Gel inhomogeneity

Regarding the gel inhomogeneity observed in depth, it was still present whatever the jar's orientation and position in the MRIdian field of view. Similarly, upside-down solidification did not remove this inhomogeneity. R2 maps of a partially filled and fully filled gel jars are shown in Fig. 4. The partially filled gel jar displays inhomogeneity in its upper part. Conversely, the fully filled gel jar shows no such inhomogeneity. Relative R2 variations are around 3.5% for the partially filled gel, compared with less than 1% for the fully filled gel. A slight increase is observed in the last 2 cm before the bottom of the jar for both configurations which may be due to the proximity of the jar edges. The R2 variations in the fully filled gel appear considerably reduced, eliminating the inhomogeneity previously observed with this new gel

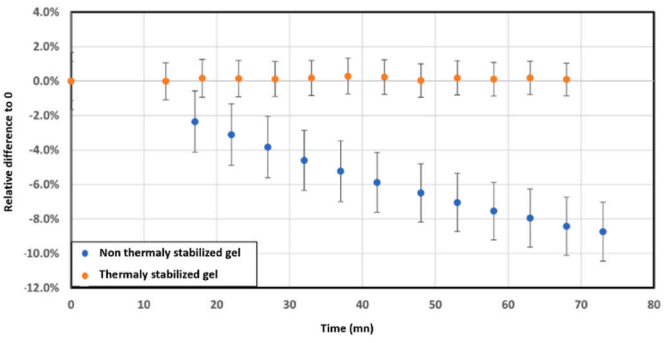


**Fig. 3.** R2 variation in time for non-irradiated gel non and pre-thermally stabilized.

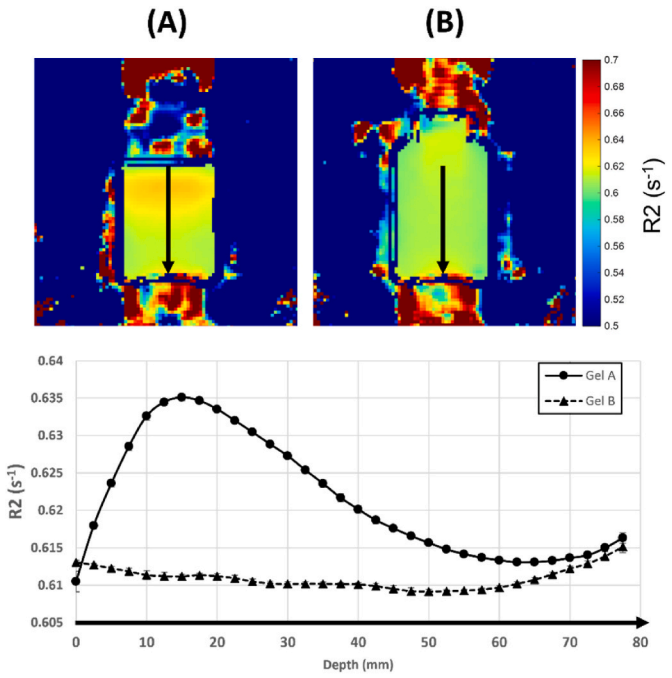


**Fig. 4.** Partially (A) and fully (B) filled unirradiated gels R2 maps and measured absolute R2 variation along the jars.

conditioning method. Additionally, it must be underlined that the presented measurements start at the same spatial position in the MRI field of view. This position corresponds to the air/gel interface for the partially filled jar but does not align with an interface for the fully filled jar. However, artifacts are present in the fully filled gel section near the jar cap where a slight increase in R2 values is observed. To our knowledge, such inhomogeneity in unirradiated Fricke gels has not been reported yet in the literature. Polymer gels are known to behave similarly and must be made under controlled atmosphere to avoid dioxygen absorption into the gel. Also, the cooling process of the gel may lead to inhomogeneity due to the delay in reaching freezer temperature between regions of the gel volume (Coulaud, 2021). In our experimentation, both gels faced the same cooling process, but removing the air from the jar during the cooling process eliminated the inhomogeneity. This could indicate that the inhomogeneity is perhaps linked to a chemical change in the region of the gel close to the interface with the air.

### 3.2. Dose response

ΔR2 map and dose distribution of the four gels are shown on Fig. 5. The four jars were arranged from left to right in the image sequence: 5 Gy calibration gel, gel irradiated with a simple plan, 3 Gy calibration gel, and 7 Gy calibration gel.

Fig. 6 shows the ΔR2 values measured along the gel calibration vials and the calibration curve established. A slight offset in ΔR2 is observed for the gel irradiated at 3 Gy during the calibration with respect to the gels irradiated to 5 Gy and 7 Gy; therefore, calibration was performed using only the gels irradiated at 5 Gy and 7 Gy. The linear fitting approach accurately represents the ΔR2 vs. dose relationship. The intersection region between the two measurements sets corresponds to measurements taken at the extremes of the two gel jars, potentially explaining the differences observed in ΔR2 between the two calibration gels that may have been originated from artifacts at these extreme

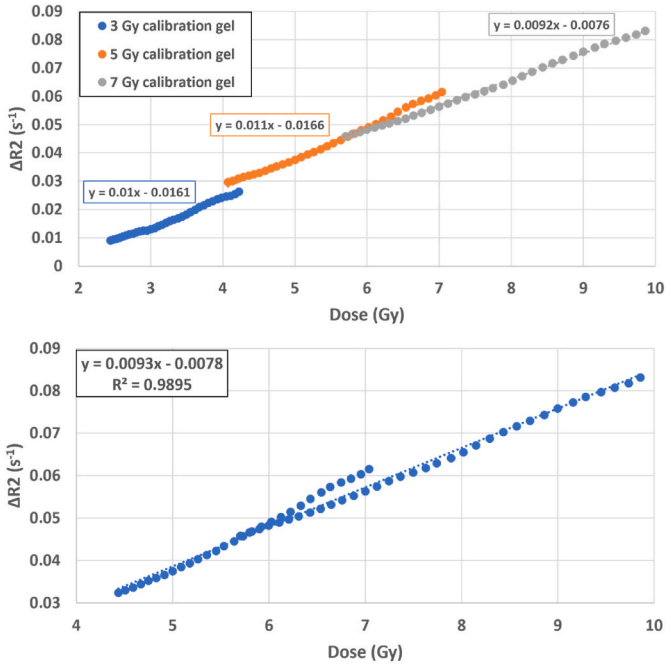


**Fig. 6.** ΔR2 values measured along gels used for calibration against TPS planned dose (top) and remaining ΔR2 values effectively used for calibration after 3 Gy gel removal (bottom) as well as the linear relationship established after regression.

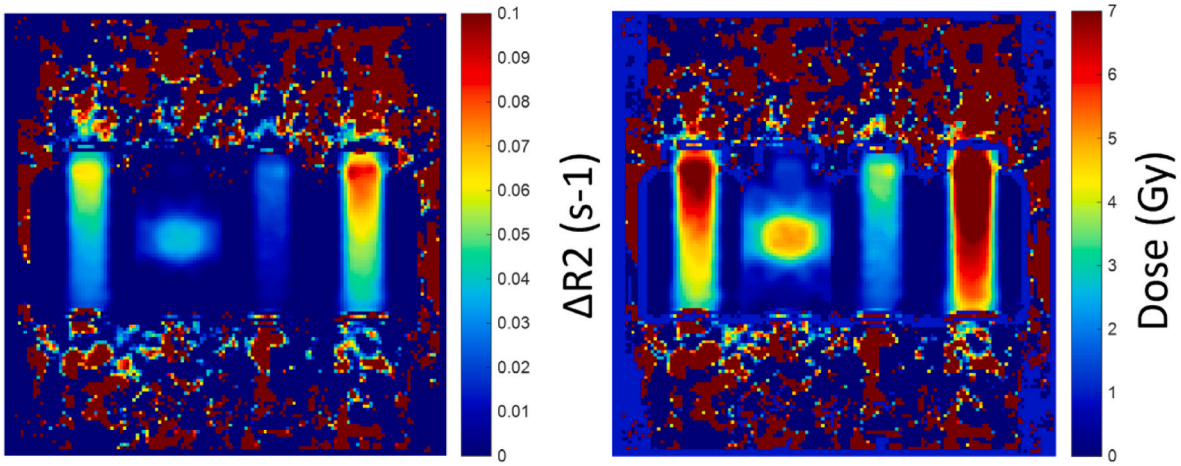


**Fig. 5.** ΔR2 (left) and converted dose map of the gels (right).

locations. The negative intercept means that the gels may have undergone a thermal shift between the pre and post irradiation readings. This negative intercept may not be a problem for dose conversion if the fourth gel has undergone the same thermal drift as the calibration gels. Nevertheless, this shift remains small thanks to the thermal stabilization protocol. Also, for the 3 Gy calibration gel, an intra-batch variability may be responsible for the higher offset encountered with the two other calibration vials. The sensitivity itself of the TruView gel is evaluated at 0.0093 $s^{-1}$. $Gy^{-1}$. This sensitivity depends on the different chemicals in the gel composition, and it was shown by (Penev and Mequanint, 2017) that the addition of 5-nitro-1,10-phenanthroline (Nn) and glyoxal (Gx) as stabilizers for diffusion and auto-oxidation, led to a lower sensitivity of the gel in optical reading in comparison with their removal from the gel composition. Additionally, the low concentration of ferrous ion (0.1 Mm) in comparison with other studies may be responsible for the low sensitivity of the gel through MRI reading since its response is proportional to changes in paramagnetic properties of these ions (De Deene, 2022).

### 3.3. 1D validation

Fig. 7 represents the dose profiles measured within the gel irradiated according to the simple plan. The measured profiles align well with those calculated by the TPS at the dose maximum. Points within the central region overall meet the 3%/3 mm criteria. However, significant differences are observed in regions outside the steep gradient, notably an overestimation in the horizontal (B) dose profile in outer regions and an underestimation in the vertical (A) dose profile. The overestimation in the horizontal (B) profile could stem from edge effects altering the R2 values in that gel region. As the diameter of the jar is smaller than its height, the effective measurement surface is reduced in these areas. Regarding the vertical profile (A), underestimation occurs over a substantial portion outside the plateau, despite the 1 cm exclusion region around the edges. These underestimations could be attributed to calibration. Specifically, the calibration gel irradiated at 3 Gy was not taken into account and ΔR2 values in the gel irradiated at 5 Gy were only measured up to 1 cm from the jar's bottom before edge phenomena distorted the maps. Consequently, calibration was limited to a dose range from 4 Gy up to 10 Gy, while regions converted below 4 Gy in the gel irradiated per the simple plan were extrapolated from the calibration. For both measured profiles, underestimation is observed at shoulder level leading to a shortening of the dose plateau and a softening of the gradient. This phenomenon is observed in both profiles, including in the calibration dose range (4–5 Gy), and may originate from diffusion of ferric ions leading to a loss of spatial integrity in the dose map.

### 3.4. 2D validation

Fig. 8 presents the calculated and measured dose maps along with the associated global gamma map using the 5%/3 mm criterion. 86.8% and 68.6% of points pass the global gamma and local gamma evaluation respectively in the selected region, excluding the volume within 1 cm of the jar walls. Points failed the criterion in the lower gel region and the gel cap region. Concerning the target volume, most of the points failing the gamma criterion are located in the dose gradient region. The remaining gel volume shows good agreement with TPS planning for doses between 1.5 and 4 Gy. Doses measured below 1.5 Gy are poorly evaluated with the gel and are likely due to inadequate calibration for the lower doses in this study as mentioned previously in the 1D dose profiles analysis.

### 3.5. Discussion

The dosimetric evaluation performed with the TruView gel on the MRIdian low field MRI is promising.

The observed specific temperature sensitivity of TruView gels,

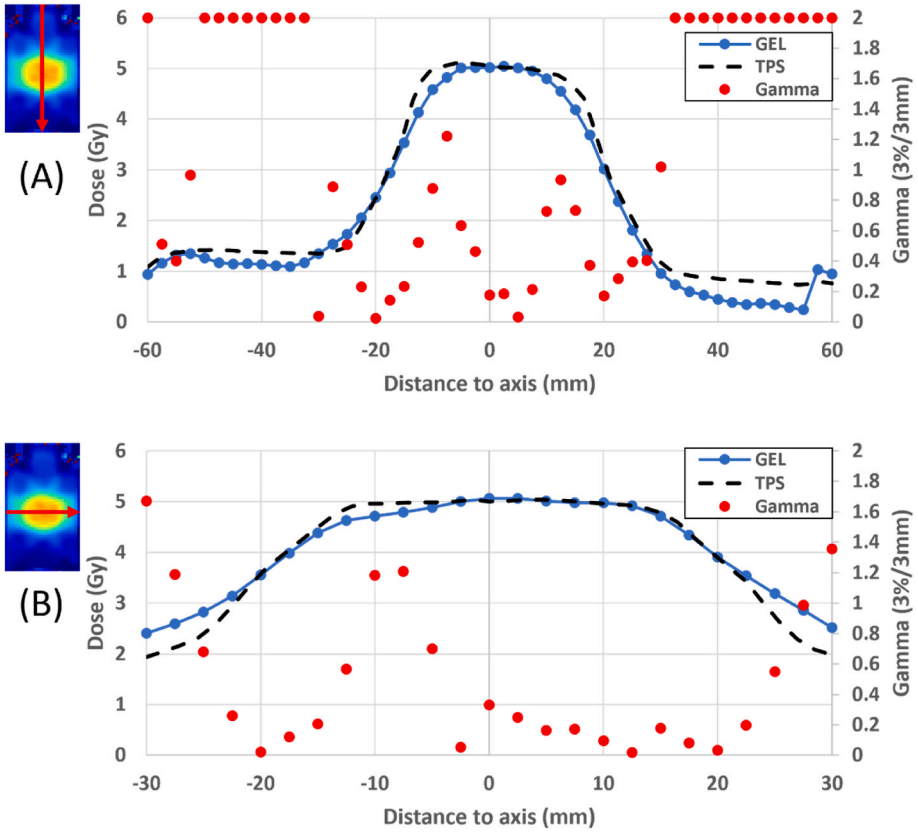


**Fig. 7.** Y (A) and X (B) dose profiles measured on the fourth gel irradiated according to the simple plan compared to TPS planned dose distributions.

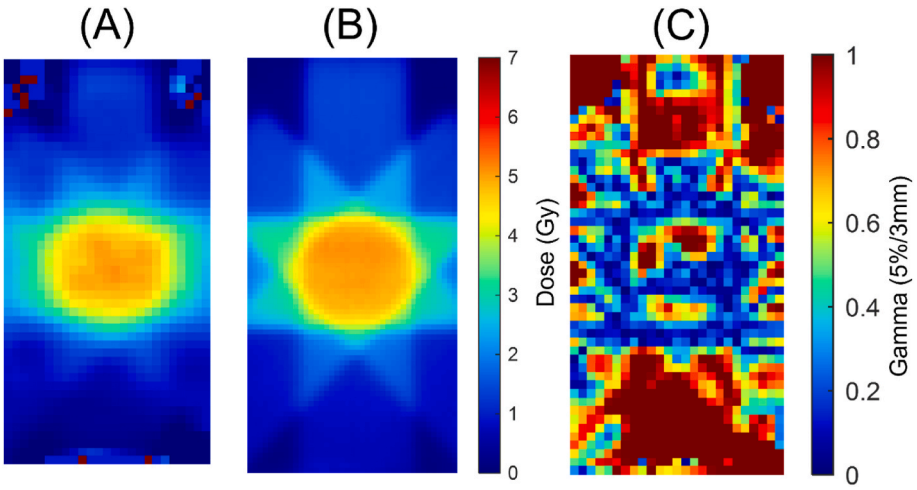


**Fig. 8.** Measured (A) and planned (B) dose maps, and global gamma map (C).

although contained by the thermal stabilization protocol implemented prior to irradiation, resulted in the inability to use the calibration gel irradiated at 3 Gy for the dosimetric evaluation. This issue stems mainly from the lower relaxometric sensitivity of the TruView gel compared with other available radiochromic gels (Marrale and d'Errico, 2021). As it stands, this low sensitivity of the TruView gel must be compensated for by robust protocols to limit drifts on converted dose maps, adding complexity to the overall protocol. A reformulation of the TruView gel by increasing $Fe2+$ ion concentration or replacing the gel matrix with PVA (Collura et al., 2018; Gallo et al., 2019, 2024; Lazzeri et al., 2019; Marrale et al., 2017; Scotti et al., 2022), combined with the removal of Nn and GX from its composition, should theoretically increase its relaxometric sensitivity (Rabaeh et al., 2018) while retaining limited diffusion phenomena (Lazzeri et al., 2019), and so, would limit the impact of thermal shifting on converted dose maps. The measured profiles showed deviations from TPS planning, but no preferential direction towards a particular gel region was observed, confirming the effectiveness of conditioning and background subtraction from reference image acquisitions in mitigating inhomogeneity effect on converted dose maps. Pappas et al. (2019); Nierer et al. (2022) did not use calibration for dose conversion in order to limit the propagation of errors on the converted maps; instead, they normalized the R2 maps to mean values scored in PTV that allow relative dose distributions to be obtained. This method simplifies the whole measurement process but requires a large dose/R2 linearity range of the gel to cover the entire distribution and a decrease in the gel's dosimetric detection threshold. It should be emphasized, that direct normalization of R2 values also leads to a reduction in the uncertainty linked to the overall calibration process that may arise from both image acquisition and intrabatch variability and is of great interest in the aim of dosimetry on low field MR-Linac. The study by (Maraghechi et al., 2020) is the only one to have addressed the evaluation of uncertainties in a gel measurement protocol on the MRIdian. They demonstrated that filtering combined with repetitions achieved an uncertainty equivalent to that of 1.5 T MRI. Thanks to the choice of acquisition parameters and pre-processing of the acquired image, we were able to reach a sufficient image quality, but the voxel size would not allow robust assessment of the dose for stereotaxic treatments delivered to patients. Nevertheless, the authors underline that even a $3 \times 3$ mm$^2$ dose map with gel provides a better dosimetric evaluation than those obtained with the standard quality insurance used in clinical routine. One strategy for reducing the size of voxel maps is the use of Single Shot sequences which enable much shorter acquisition, making the measurement process viable in clinical settings. This reduction in acquisition time makes it possible to increase the image averaging and therefore the signal-to-noise ratio of the resulting image. A reduction in voxel size can then be envisaged at the cost of a longer acquisition time, that will still be kept shorter than the gold SE sequences. The study by (Nierer et al., 2022) on an anthropomorphic head phantom with a PG polymer gel is the only known study to have used the same type of sequence as ours for their acquisitions. However, they did not perform the reading directly on the MRIdian but on a 1.5 T MRI providing a higher SNR. As highlighted by the authors, this type of sequence is highly prone to artifacts, particularly in the direction of phase encoding. Consequently, these sequences require thorough characterization in order to either cancel or compensate for these artifacts for dosimetric applications.

## 4. Conclusion

This study focuses on the feasibility of reading the TruView MTB Fricke gels with the low-field MRI of the MRIdian system for dose distribution assessment. Relaxometric characterization of non-irradiated TruView gels revealed their high thermal sensitivity in relaxation times, leading to the development of a stabilization protocol. Adjustments in gel conditioning were made to reduce chemical inhomogeneities, while edge artifacts were addressed by excluding a 1 cm region at the interfaces between media. Consequently, assessment of the TruView gel's dosimetric performance was undertaken, indicating a lower relaxometric sensitivity in R2 than other Fricke gels. Post-irradiation measurements were refined by subtracting post-irradiation images from those acquired prior to irradiation to mitigate inhomogeneities and artifacts. Rather good agreement was observed between measured and TPS profiles; however, discrepancies were observed in the dose gradient and were attributed to diffusion phenomena. 2D validation by gamma comparison with TPS planning displayed overall agreement, with the exceptions of regions with strong dose gradients This comprehensive analysis emphasizes the need for precise calibration methods, and optimization of gel sensitivity for reliable dosimetric evaluations. Complete characterization of the MRI sequences used, especially complex sequences such as the single shot, is imperative to minimize artifacts impacting relaxometric maps. The integration of MRI/Linac coupling eliminated gel repositioning uncertainties and minimized variabilities induced by gel inhomogeneities, offering a significant advantage over traditional Linacs. Optimizing image acquisition sequences and pre-processing facilitated the acquisition of quality relaxometric maps, substantially reducing evaluation times and allows for realistic clinic dosimetry evaluation implying Fricke gel dosimetry on low magnetic field MR-Linac. Finally, a 3D dosimetric validation of the developed protocol must be carried out to enable its application as a robust tool for patient QA. Particular attention

will need to be paid to the specific artifacts observed due to the MRIdian's gradient design, which must be compensated for prior to the implementation of SNR/time efficient 3D quantitative sequences (Marage et al., 2023).

## CRediT authorship contribution statement

**L. Ermeneux:** Writing – original draft, Methodology, Formal analysis. **A. Petitfils:** Writing – review & editing, Methodology. **L. Marage:** Writing – review & editing, Methodology. **R. Gschwind:** Writing – review & editing, Supervision, Methodology. **C. Huet:** Writing – original draft, Supervision, Methodology, Formal analysis, Conceptualization.

## Declaration of competing interest

The authors declare that they have no known competing financial interests or personal relationships that could have appeared to influence the work reported in this paper.

## Data availability

Data will be made available on request.

## References


Baldock, C., De Deene, Y., Doran, S., Ibbott, G., Jirasek, A., Lepage, M., McAuley, K.B., Oldham, M., Schreiner, L.J., 2010. Polymer gel dosimetry. Phys. Med. Biol. 55 https://doi.org/10.1088/0031-9155/55/5/R01.

Baldock, C., Karger, C.P., Zaidi, H., 2020. Gel dosimetry provides the optimal end-to-end quality assurance dosimetry for MR-linacs. Med. Phys. 47, 3259–3262. https://doi.org/10.1002/mp.14239.

Chou, Y.-H., Lu, Y.-C., Peng, S.-L., Lee, S.-C., Hsieh, L.-L., Shih, C.-T., 2020. Evaluation of the dose distribution of tomotherapy using polymer gel dosimeters and optical computed tomography with ring artifact correction. Radiat. Phys. Chem. 168, 108572 https://doi.org/10.1016/j.radphyschem.2019.108572.

Collura, G., Gallo, S., Tranchina, L., Abbate, B.F., Bartolotta, A., d'Errico, F., Marrale, M., 2018. Analysis of the response of PVA-GTA Fricke-gel dosimeters with clinical magnetic resonance imaging. Nucl. Instrum. Methods Phys. Res. B 414, 146–153. https://doi.org/10.1016/j.nimb.2017.06.012.

Colnot, J., Huet, C., Clairand, I., 2017. Characterisation of TruView$^{TM}$: a new 3-D reusable radiochromic MethylThymolBlue based gel dosimeter for ionising radiations. J Phys Conf Ser 847, 012017. https://doi.org/10.1088/1742-6596/847/1/012017.

Colnot, J., Huet, C., Gschwind, R., Clairand, I., 2018. Characterisation of two new radiochromic gel dosimeters TruView$^{TM}$ and ClearView$^{TM}$ in combination with the vista$^{TM}$ optical CT scanner: a feasibility study. Phys. Med. 52, 154–164. https://doi.org/10.1016/j.ejmp.2018.07.002.

Coulaud, J., 2021. Sécurisation des traitements radiothérapeutiques du cancer : validation physique des plans théoriques de radiothérapie par des fantômes dosimétriques anthropomorphes To cite this version : HAL Id : tel-03148804.

da Silveira, M.A., Pavoni, J.F., Bruno, A.C., Arruda, G.V., Baffa, O., 2022. Three-dimensional dosimetry by optical-CT and radiochromic gel dosimeter of a multiple isocenter craniospinal radiation therapy procedure. Gels 8, 582. https://doi.org/10.3390/gels8090582.

De Deene, Y., 2022. Radiation dosimetry by use of radiosensitive hydrogels and polymers: mechanisms, state-of-the-art and perspective from 3D to 4D. Gels 8, 599. https://doi.org/10.3390/gels8090599.

De Deene, Y., De Wagter, C., 2001. Artefacts in multi-echo T2 imaging for high-precision gel dosimetry: III. Effects of temperature drift during scanning. Phys. Med. Biol. 46, 2697–2711. https://doi.org/10.1088/0031-9155/46/10/312.

Doran, S.J., Koerkamp, K.K., Bero, M.A., Jenneson, P., Morton, E.J., Gilboy, W.B., 2001. A CCD-based optical CT scanner for high-resolution 3D imaging of radiation dose distributions: equipment specifications, optical simulations and preliminary results. Phys. Med. Biol. 46, 3191–3213. https://doi.org/10.1088/0031-9155/46/12/309.

Dorsch, S., Mann, P., Elter, A., Runz, A., Spindeldreier, C.K., Klüter, S., Karger, C.P., 2019. Measurement of isocenter alignment accuracy and image distortion of an 0.35 T MR-Linac system. Phys. Med. Biol. 64 https://doi.org/10.1088/1361-6560/ab4540.

Elter, A., Dorsch, S., Marot, M., Gillmann, C., Johnen, W., Runz, A., Spindeldreier, C.K., Klüter, S., Karger, C.P., Mann, P., 2022. RSC: gel dosimetry as a tool for clinical implementation of image-guided radiotherapy. J Phys Conf Ser 2167. https://doi.org/10.1088/1742-6596/2167/1/012020.

Fricke, H., Morse, S., 1927. The chemical action of roentgen rays on dilute ferrous sulphate solutions as a measure of radiation dose. Am. J. Roentgenol. Radium Ther. Nucl. Med. 18, 430–432.

Gallo, S., Artuso, E., Brambilla, M.G., Gambarini, G., Lenardi, C., Monti, A.F., Torresin, A., Pignoli, E., Veronese, I., 2019. Characterization of radiochromic poly (vinyl-alcohol)–glutaraldehyde Fricke gels for dosimetry in external x-ray radiation therapy. J. Phys. D Appl. Phys. 52, 225601 https://doi.org/10.1088/1361-6463/ab08d0.

Gallo, S., Locarno, S., Brambilla, E., Lenardi, C., Pignoli, E., Veronese, I., 2024. Dosimetric characterization of double network Fricke hydrogel based on PVA-GTA and phenylalanine peptide derivative. J. Phys. D Appl. Phys. 57, 075303 https://doi.org/10.1088/1361-6463/ad0987.

Gore, J.C., Kang, Y.S., 1984. Measurement of radiation dose distributions by nuclear magnetic resonance (NMR) imaging. Phys. Med. Biol. 29, 1189–1197. https://doi.org/10.1088/0031-9155/29/10/002.

Gore, J.C., Ranade, M., Maryański, M.J., Schulz, R.J., 1996. Radiation dose distributions in three dimensions from tomographic optical density scanning of polymer gels: I. Development of an optical scanner. Phys. Med. Biol. 41, 2695–2704. https://doi.org/10.1088/0031-9155/41/12/009.

Hilts, M., 2006. X-ray computed tomography imaging of polymer gel dosimeters. J Phys Conf Ser 56, 95–107. https://doi.org/10.1088/1742-6596/56/1/009.

Hilts, M., Audet, C., Duzenli, C., Jirasek, A., 2000. Polymer gel dosimetry using x-ray computed tomography: a feasibility study. Phys. Med. Biol. 45, 2559–2571. https://doi.org/10.1088/0031-9155/45/9/309.

Javaheri, N., Yarahmadi, M., Refaei, A., Aghamohammadi, A., 2020. Improvement of sensitivity of X-ray CT reading method for polymer gel in radiation therapy. Rep. Practical Oncol. Radiother. 25, 100–103. https://doi.org/10.1016/j.rpor.2019.12.017.

Jirasek, A., Marshall, J., Mantella, N., Diaco, N., Maynard, E., Teke, T., Hilts, M., 2020. Linac-integrated kV-cone beam CT polymer gel dosimetry. Phys. Med. Biol. 65, 225030 https://doi.org/10.1088/1361-6560/abbb76.

Klüter, S., 2019. Technical design and concept of a 0.35 T MR-Linac. Clin Transl Radiat Oncol 18, 98–101. https://doi.org/10.1016/j.ctro.2019.04.007.

Lazzeri, L., Marini, A., Cascone, M.G., d'Errico, F., 2019. Dosimetric and chemical characteristics of Fricke gels based on PVA matrices cross-linked with glutaraldehyde. Phys. Med. Biol. 64, 085015 https://doi.org/10.1088/1361-6560/ab135c.

Macchione, M.A., Lechón Páez, S., Strumia, M.C., Valente, M., Mattea, F., 2022. Chemical overview of gel dosimetry systems: a comprehensive review. Gels 8, 663. https://doi.org/10.3390/gels8100663.

Marage, L., Petitfils, A., Bessieres, I., Aubignac, L., Boudet, J., 2022. Feasibility study : polymer gel dosimetry on 0.35T MR-Linac system. Conference: AAPM, 2022.

Marage, L., Walker, P.-M., Boudet, J., Fau, P., Debuire, P., Clausse, E., Petitfils, A., Aubignac, L., Rapacchi, S., Bessieres, I., 2023. Characterisation of a split gradient coil design induced systemic imaging artefact on 0.35 T MR-linac systems. Phys. Med. Biol. 68, 01NT03 https://doi.org/10.1088/1361-6560/aca876.

Maraghechi, B., Gach, H.M., Setianegara, J., Yang, D., Li, H.H., 2020. Dose uncertainty and resolution of polymer gel dosimetry using an MRI guided radiation therapy system's onboard 0.35 T scanner. Phys. Med. 73, 8–12. https://doi.org/10.1016/j.ejmp.2020.04.004.

Marrale, M., Collura, G., Gallo, S., Nici, S., Tranchina, L., Abbate, B.F., Marineo, S., Caracappa, S., d'Errico, F., 2017. Analysis of spatial diffusion of ferric ions in PVA-GTA gel dosimeters through magnetic resonance imaging. Nucl. Instrum. Methods Phys. Res. B 396, 50–55. https://doi.org/10.1016/j.nimb.2017.02.008.

Marrale, M., d'Errico, F., 2021. Hydrogels for three-dimensional ionizing-radiation dosimetry. Gels 7, 74. https://doi.org/10.3390/gels7020074.

Nierer, L., Kamp, F., Reiner, M., Corradini, S., Rabe, M., Dietrich, O., Parodi, K., Belka, C., Kurz, C., Landry, G., 2022. Evaluation of an anthropomorphic ion chamber and 3D gel dosimetry head phantom at a 0.35 T MR-linac using separate 1.5 T MR-scanners for gel readout. Z. Med. Phys. 32, 312–325. https://doi.org/10.1016/j.zemedi.2022.01.006.

Oldham, M., McJury, M., Baustert, I.B., Webb, S., Leach, M.O., 1998. Improving calibration accuracy in gel dosimetry. Phys. Med. Biol. 43, 2709–2720. https://doi.org/10.1088/0031-9155/43/10/002.

Oldham, M., Siewerdsen, J.H., Shetty, A., Jaffray, D.A., 2001. High resolution gel-dosimetry by optical-CT and MR scanning. Med. Phys. 28, 1436–1445. https://doi.org/10.1118/1.1380430.

Olesen, J.L., Jespersen, S.N., 2020. About the Slightly Modified MP-PCA, vol. 142, pp. 1–7.

Pappas, E., Kalaitzakis, G., Boursianis, T., Zoros, E., Zourari, K., Pappas, E.P., Makris, D., Seimenis, I., Efstathopoulos, E., Maris, T.G., 2019. Dosimetric performance of the Elekta Unity MR-linac system: 2D and 3D dosimetry in anthropomorphic inhomogeneous geometry. Phys. Med. Biol. 64 https://doi.org/10.1088/1361-6560/ab52ce.

Penev, K.I., Mequanint, K., 2017. Multifactorial study and kinetics of signal development in ferrous–methylthymol blue–gelatin gel dosimeters. Med. Phys. 44, 1948–1957. https://doi.org/10.1002/mp.12201.

Penev, K.I., Mequanint, K., 2015. Methylthymol blue in Fricke gels. J Phys Conf Ser 573, 6–11. https://doi.org/10.1088/1742-6596/573/1/012030.

Raaymakers, B.W., Jürgenliemk-Schulz, I.M., Bol, G.H., Glitzner, M., Kotte, A.N.T.J., Van Asselen, B., De Boer, J.C.J., Bluemink, J.J., Hackett, S.L., Moerland, M.A., Woodings, S.J., Wolthaus, J.W.H., Van Zijp, H.M., Philippens, M.E.P., Tijssen, R., Kok, J.G.M., De Groot-Van Breugel, E.N., Kiekebosch, I., Meijers, L.T.C., Nomden, C. N., Sikkes, G.G., Doornaert, P.A.H., Eppinga, W.S.C., Kasperts, N., Kerkmeijer, L.G. W., Terssteeg, J.H.A., Brown, K.J., Pais, B., Woodhead, P., Lagendijk, J.J.W., 2017. First patients treated with a 1.5 T MRI-Linac: clinical proof of concept of a high-precision, high-field MRI guided radiotherapy treatment. Phys. Med. Biol. 62, L41–L50. https://doi.org/10.1088/1361-6560/aa9517.

Rabaeh, K.A., Eyadeh, M.M., Hailat, T.F., Aldweri, F.M., Alheet, S.M., Eid, R.M., 2018. Characterization of ferrous-methylthymol blue-polyvinyl alcohol gel dosimeters using nuclear magnetic resonance and optical techniques. Radiat. Phys. Chem. 148, 25–32. https://doi.org/10.1016/j.radphyschem.2018.02.019.

Rae, W., Willemse, C., Lötter, M., Engelbrecht, J., Swarts, J., 1996. Chelator effect on ion diffusion in ferrous-sulfate-doped gelatin gel dosimeters as analyzed by MRI. Med. Phys. 23, 15–23. https://doi.org/10.1118/1.597787.

Scotti, M., Arosio, P., Brambilla, E., Gallo, S., Lenardi, C., Locarno, S., Orsini, F., Pignoli, E., Pedicone, L., Veronese, I., 2022. How xylenol orange and ferrous ammonium sulphate influence the dosimetric properties of PVA–GTA Fricke gel dosimeters: a spectrophotometric study. Gels 8, 204. https://doi.org/10.3390/gels8040204.

Turner, R., Streicher, M., 2012. Measuring temperature using MRI: a powerful and versatile technique. Magnetic Resonance Materials in Physics. Biol. Med. 25, 1–3. https://doi.org/10.1007/s10334-011-0299-y.